Effect of hydrogen absorption on the cerium electronic state in $CeFe_{11}Ti$: An x-ray-absorption and circular-magnetic-dichroism investigation

Jesús Chaboy
Instituto de Ciencia de Materiales de Aragon, 50009 Zaragoza, Spain

Augusto Marcelli
Istituto Nazionale di Fisica Nucleare, Laboratori Nazionali di Frascati, Cassella Postale 13, 00044 Frascati, Italy

Latchezar Bozukov
Faculty of Physics, Sofia University, 1126 Sofia, Bulgaria

Francois Baudelet
Laboratoire de Physique des Solides, Université de Nancy I, 54506 Vandoeuvre-les-Nancy, France and Laboratoire pour l'Utilisation du Rayonnement Electromagnétique, Batiment 209D, Université Paris-Sud, 91405 Orsay, France

Elisabeth Dartyge, Alain Fontaine, and Stefania Pizzini
Laboratoire pour l'Utilisation du Rayonnement Electromagnétique, Batiment 209D, Université Paris-Sud, 91405 Orsay, France
(Received 1 August 1994)

We present a combined x-ray-absorption-spectroscopy (XAS) and x-ray-circular-magnetic-dichroism (XCMD) study performed on the $CeFe_{11}TiH_x$ systems. Looking at the changes of the local structure around the metal atoms by EXAFS (extended x-ray-absorption fine structure), the crystallographic position occupied by hydrogen in these compounds has been inferred. Moreover, the influence of hydrogen into the intermediate-valence state of Ce and the electronic localization is discussed. Both XAS and XCMD results evidence the strong correlation between the structural and magnetic changes associated with the modification of the hybridization between the Fe $3d$ and Ce $5d$ bands.

I. INTRODUCTION

The discovery of the novel $R_2Fe_{14}B$ materials, in which R is a rare-earth element, has recently renewed permanent magnet research.[1,2] The ternary compound $Nd_2Fe_{14}B$ exhibits both superior hard-magnet properties and economic advantages over the earlier Sm-Co materials and has stimulated intensive studies of iron-rich ternary compounds based on rare earths. However, the range of temperature in which these new alloys are of technological significance is strongly limited because ordering temperatures T_c are sufficiently low to render them unsuitable for some applications. The need to improve their hard-magnet performance has triggered worldwide efforts to synthesize novel materials in the large group of ternary phases.

Among the large number of rare-earth-based intermetallics, interest has recently focused on pseudobinaries with the $ThMn_{12}$ structure, $R(Fe_{12-x}M_x)$. Although the pure end member RFe_{12} does not exist for any rare earth, the structure has been stabilized for M=Ti, V, Cr, Mo, W, and Al.[3–6] In particular, special attention has been devoted to the study of the R-Fe-Ti phases because early investigations reported the existence of strong uniaxial anisotropy in Sm-based compounds and in the case of $SmFe_{11}Ti$ the ordering temperature is close to that of $Nd_2Fe_{14}B$.[7] Nowadays, one of the main efforts to improve the hard-magnet properties of these materials is devoted to increase their T_c, with the most outstanding being the interstitial solution of H, N, or C atoms. Indeed, the increase of the Curie temperature and saturation magnetization is sometimes coupled to a drastic change of the magnetocrystalline anisotropy, resulting in a surprisingly high hardness development, making these interstitial compounds suitable candidates for permanent-magnet applications.[8]

The impact of the interstitial solutions on the magnetic properties is specially interesting in the case of the Ce-based compounds. Such a class of compounds exhibits an additional effect due to hydrogen absorption that concerns the modification of the cerium electronic configuration. A common result to all the R-Fe series investigated to date is related to the existence within each different series of anomalously smaller lattice parameters for the Ce-based compounds. This trend has been largely associated with the presence of cerium in the Ce^{4+} electronic state in these alloys. After H_2 uptake, cerium-based alloys show the highest relative volume increase and lattice parameter expansion, leading to a considerable reduction of the mentioned anomalies. Previous works interpreted these findings in terms of a Ce valence change from tetravalency to trivalency induced by hydrogen.[9–11]

However, other experimental indications do not support this interpretation on the interplay between cerium valence and hydrogen absorption.[12] The understanding of this controversy is one of the main motivations of this research.

We report in the present work an extensive x-ray-absorption-spectroscopy (XAS) and x-ray-circular-magnetic-dichroism (XCMD) study on $CeFe_{11}Ti$ and $CeFe_{11}TiH_x$ systems. The local environment of the iron and titanium atoms has been investigated by extended x-ray-absorption fine structure (EXAFS) to infer the crystallographic position occupied by the hydrogen atoms. On the other hand, the valency state of cerium has been investigated by x-ray-absorption near-edge structure (XANES) at the Ce L_3 edge. In addition, measurements of the cerium L_1-edge and Fe K-edge XANES spectra together with XCMD spectra at both the Fe K edge and at the Ce $L_{2,3}$ edges have been performed. Indeed, XAS and XCMD experiments performed at different edges and different atomic species make possible the reconstruction of the local and partial density of states around the Fermi energy. In these systems, such a combined analysis shows electronic localization phenomena that clearly address the change in the magnetic properties of the systems upon hydriding to the modification of the $3d$(Fe)-$5d(R)$ hybridization. Moreover, the relationship between hydrogen absorption and cerium electronic state in these iron-rich intermetallics compounds is discussed.

II. EXPERIMENTAL SETUP

The $CeFe_{11}Ti$ samples were prepared by arc melting of Ce, Fe, and Ti (99.9% purity) under a purified Ar atmosphere followed by vacuum homogenization at 1273 K for 1 week. Both phase and structural analyses were performed on a standard x-ray diffractometer. The hydrogen-absorption and -desorption properties were established at the hydrogen pressure of 0.1–4 $\times$ 10^3 kPa in the temperature range of 270–570 K by a volumetric automated experimental setup described elsewhere.[13,14]

XAS experiments have been performed at the iron and titanium K edge and at the $L_{1,3}$ edges of cerium in $CeFe_{11}Ti$ and $CeFe_{11}TiH_{0.8}$ compounds. Several samples were measured in different experimental runs at the PULS synchrotron radiation facility of the Laboratory Nazionali di Frascati. The ADONE storage ring was operated at 1.5 GeV during dedicated beam time with an averaged current of approximately 40 mA. The x-ray radiation was monochromatized using a Si(111) channel-cut crystal.

XCMD spectra were recorded at LURE, using an energy-dispersive-based spectrometer for XAS experiments in transmission geometry associated with a position-sensitive detector. The absorption spectra were recorded by selecting the beam at 0.4 mrad below the orbit plane, yielding a rate of about 0.7 right circularly polarized light. The procedure of data collection and the experimental setup are described elsewhere.[15]

All the absorption experiments were carried out at room temperature in the transmission mode; both x rays incident on the sample and transmitted through it were monitored with two independent ionization chambers using flowing gas (N_2, Ar) mixtures optimized for each different energy range. Samples were held in vacuum and formed by homogeneous thin layers. The total thickness was chosen to optimize the signal-to-noise ratio. During each experimental run, both fresh and old samples were measured to establish the stability of hydrogen content. No appreciable difference, other than the signal-to-noise ratio, was ever observed.

III. RESULTS AND DISCUSSION

A. Fe and Ti K-edge EXAFS

The absorption spectra were analyzed according to standard procedures.[16] The background contribution from previous edges $\mu_B(E)$ was fitted with a linear function and subtracted from the experimental spectrum $\mu(E)$. The average absorption above the edge was fitted with a smooth spline formed by three cubic polynomials to simulate the atomiclike term $\mu_0(E)$. The EXAFS signal $\chi(k)$ was then determined as $\chi(k) = (\mu - \mu_B - \mu_0)/\mu_0$, where the photoelectron wave vector k is defined by $k = \sqrt{(2m/\hbar^2)(E - E_0)}$. The energy origin E_0, corresponding to the continuum threshold, was defined to be at the inflection point of the absorption edge.

The EXAFS oscillations at the Ti K edge obtained in this way are reported in Fig. 1 for the $CeFe_{11}Ti$ and $CeFe_{11}TiH_{0.8}$ samples, together with the corresponding Fourier transforms over the K range $2.2 \leq k \leq 10$ Å^{-1}. Note that the phase correction was not included in the Fourier transform (FT); therefore the peak positions are shifted from their true values.[17]

The comparison of the local structure around titanium, substituting Fe at the ($8i$) sites (see Fig. 2), prior and after the hydrogen uptake shows that the crystal structure is retained, in agreement with previous observations.[13] Indeed, the modulation of the EXAFS signals is near identical, the smoothing of the EXAFS structures for the hydride derivative indicating a slight increase in the atomic disorder induced by H_2. In addition, a more detailed inspection of the EXAFS spectra leads to a deeper insight about the crystallographic position occupied by hydrogen. The quality of the data allows, in the case of the hydride derivative, the identification of a small shift of the FT peaks located at $R \leq 2.6$ Å toward lower R values. It indicates the contraction of all the interatomic distances smaller than 3 Å around the absorbing Ti atom. On the contrary, an opposite behavior for the FT peaks at the higher distances, which reflects a weak expansion of the crystal lattice.

This behavior is extremely important to understand the weak modifications occurring upon hydriding in such structure. In fact, two different positions for the H_2 location in the crystal cell have been proposed to date. Obbade *et al.* discussing this problem in relation to the $RFe_{12-x}M_x$ series (R=Y,Nd; M=Ti,V), reported a preferential hydrogen occupancy of the $R(2a)$-Ti($8i$)-Fe($8i$)-Fe($8j$) tetrahedra, Fig. 2.[18] On the contrary, more recent

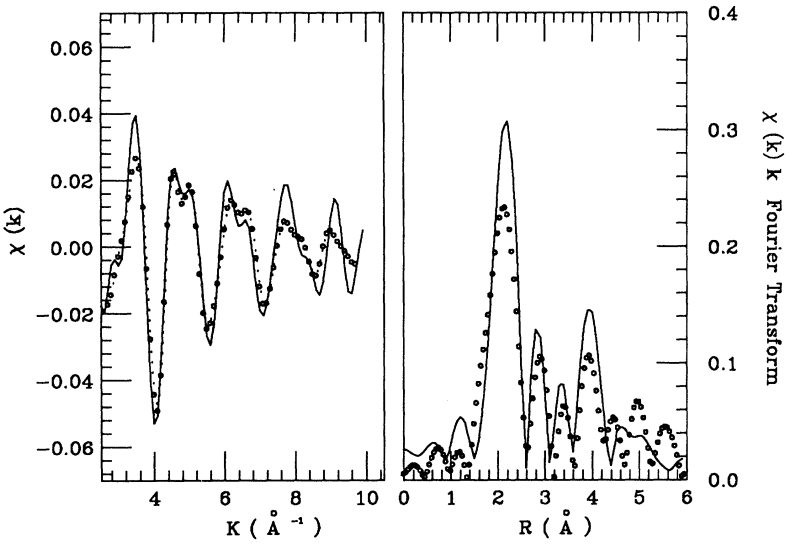

FIG. 1. Ti K-edge EXAFS spectra for both $CeFe_{11}Ti$ (solid line) and $CeFe_{11}TiH_{0.8}$ (dots) systems (left panel). The $k\chi(k)$ signals were Fourier transformed in the range $2.2 \leq k \leq 10$ Å^{-1} by using a Hanning window function (right panel).

results identify it with the (2b) octahedral position, being formed by two rare-earth atoms and four iron ($8j$) atoms.[19] The presence of H atoms in these two alternative locations would induce a different deformation of the crystal cell. In this sense, the occupancy of the tetrahedral positions leads to a uniform distortion around the Ti site propagating along the basal (z=0) plane. This effect implies the expansion of the interatomic distances around the titanium site and, in particular, the increment of the shortest Ti-Fe distance, corresponding to one Fe($8j$) atom in the z=0.5 plane, is expected. However, this prediction is not supported by our EXAFS results that show just the contraction of the Ti next-nearest-neighbor distances and thus support the hypothesis of the occupancy of the octahedral ($2b$) positions by hydrogen. Indeed, *ab initio* EXAFS simulations performed by using theoretical phase shifts and scattering amplitudes calculated by the *FEFF* code[20] report a 0.03 Å contraction of the shortest Ti-Fe interatomic distance in the hydride derivative.

Trying to solve this controversy, making use of the atomic selectivity of the EXAFS technique, a similar

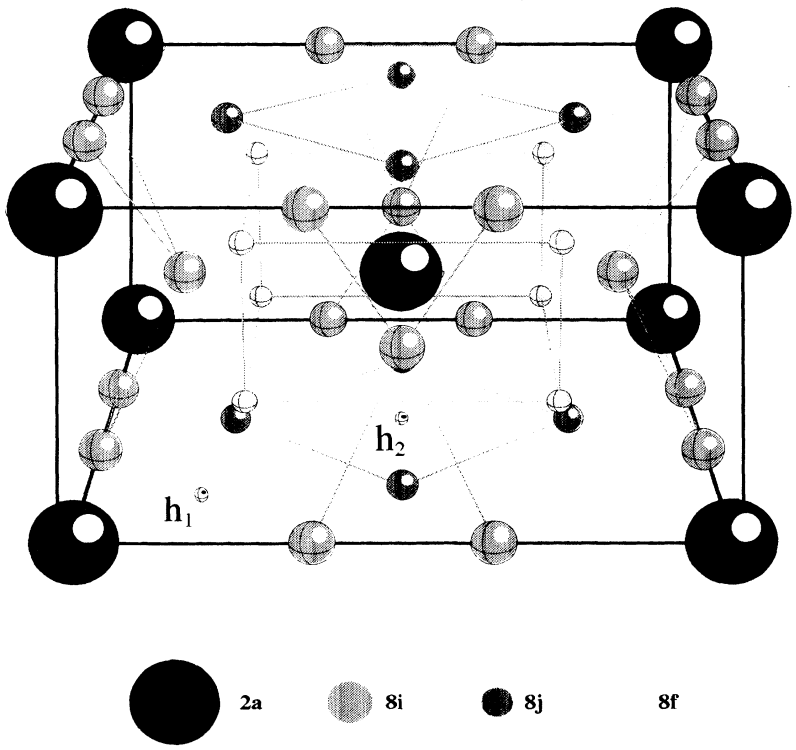

FIG. 2. Crystallographic structure for the $CeFe_{11}TiH_x$ system (left panel). Two different positions are pointed for the preferential hydrogen occupancy according to recent published results (Refs. 18 and 19).

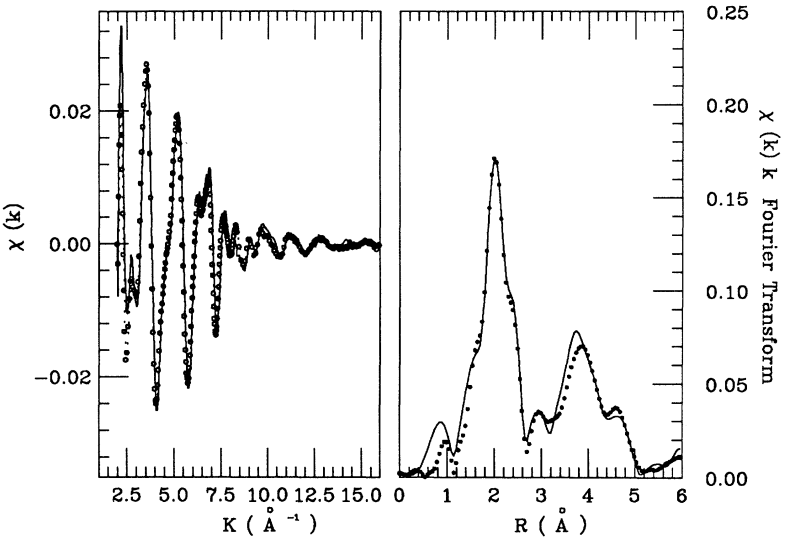

FIG. 3. Extracted iron K-edge EXAFS signals in $CeFe_{11}Ti$ (solid line) and $CeFe_{11}TiH_{0.8}$ (dots) compounds. The corresponding k-weighted Fourier transforms are shown in the right panel.

analysis has been performed on the EXAFS signals at the Fe K edge. The $k\chi(k)$ signals and their Fourier transforms over the range $2.5 \leq k \leq 14$ Å^{-1} are reported in Fig. 3. At this edge, the most intense structure contributing to the FT arises from the scattering of the photoelectron with the Ti and Fe atoms located in the same plane at ~2.6 Å from the absorber. Upon hydrogenation a small contraction of these distances is observed. However, in the case of Fe the EXAFS signal is due to the superposition of the contributions coming from the three different Fe sites, in such a way that the total signal only reflects an average of the distortion. Nevertheless, best fits to the experimental spectra of the theoretical $FEFF$ signals,[20,21] evidence the increase of the shortest Fe($8j$)-Fe($8f$) distance, corresponding to Fe atoms located at the z=0.5 and z=0.25 planes, respectively, as expected from a distortion proceeding along the z axis as that driven by the hydrogen filling of the ($2b$) octahedral sites.

Additional phenomenological considerations support this occupational scheme, filling the octahedral $2b$ sites, for hydrogen. Indeed, the maximum hydrogen content observed in the $RFe_{11}M$ series never exceeds 1 H atom/f.u. which agrees with the available number of ($2b$) sites in the crystal cell. Furthermore, the octahedral sites have the shortest distance from the rare earth among all the empty interstitial sites and, because of the large electronegativity difference between hydrogen and rare earth, it must be more preferential and more stable for hydrogen to occupy the $2b$ sites. In addition, it is important to emphasize that the octahedral interstice is larger than the tetrahedral one and coordinates two rare-earth atoms along the z axis. This occupancy hypothesis would also explain why the distortion is larger along the c axis than in the basal plane, leading to the observed reduction of the a/c ratio upon hydriding in $RFe_{11}Ti$.

B. Mixed-valence behavior: Ce L_3-edge XANES spectra

The structural modifications induced by hydrogen are undoubtedly linked to the changes in the magnetic properties occurring in these systems upon hydriding. In fact, the magnetic ordering temperature increases from 503 to 553 K in the case of $CeFe_{11}TiH_x$ whereas the magnetization presents a 5% enhancement.[13] Such behavior is comparable to that of the rest of the series in which the increase in T_c ranges between 40 and 50 K and the saturation magnetization rises 4% in $YFe_{11}TiH_x$.[23]

The rise of the ordering temperature upon interstitial doping of H, C, and N atoms is a common, but not clearly understood, effect shared by all rare-earth iron-rich intermetallic compounds. Apparently, a connection between the expansion of the crystal lattice and the rise in T_c could be considered. In fact, despite the relative proximity of the average Fe moment in these compounds and in elemental Fe, the ordering temperatures are substantially smaller, T_c(Fe)=1043 K. This behavior has been assigned to the strong sensitivity of the Fe-Fe exchange interactions to the Fe-Fe separation, in such a way that for distances smaller than 2.5 Å antiferromagnetic exchange is expected resulting in lower Curie temperatures.[22] In particular, many authors argue that the T_c increase after hydriding is simply due to the expansion of the lattice parameters because of the reduction of the negative exchange interaction resulting from the shortening of the Fe-Fe separation.[9,10,23–26]

In addition, in the case of Ce-based materials several reports have addressed the anomalously high increase of the lattice parameters upon hydriding to a tetravalent-trivalent change in the valency of cerium that would be also at the origin where the magnetic changes occurred.[9,10,26,27,11] Despite the unclear relationship between volume and valence, these studies deal with analyses of lattice parameters and volume anomalies correlating them to the valence change of cerium upon hydriding. Actually, the assignment of cerium electronic configuration is made on the grounds of the anomalously small lattice parameters of the Ce material as compared with the other R-based alloys. Typical examples are found in the $R_2Fe_{14}B$ and R_2Fe_{17} series: The crystal cell volume of $Ce_2Fe_{14}B$ and Ce_2Fe_{17} compounds are, respectively, 1.98% and 2.16% smaller than those of the Nd compounds, whereas upon hydriding the relative volume

ratio between the Ce- and Nd-based alloys diminishes to 0.82% and 0.66%, respectively. However, the unknown nature of the configuration mixing and the lack of reliable models for the Ce^{4+} ion raise questions about the validity of conclusions based exclusively on such analyses.[28]

The investigation of the $CeFe_{11}TiH_x$ systems offers a good challenge to verify the validity of these hypothesis: (i) The increase in the ordering temperature is due to the reduction of the negative exchange associated with the expansion of the shortest Fe-Fe distances, and (ii) the existence of Ce in a pure tetravalent configuration and thus the possible change of cerium valency from Ce^{4+} to Ce^{3+} upon H_2 uptake. To this aim we have performed experiments at the cerium L_3-absorption edge in both $CeFe_{11}Ti$ and $CeFe_{11}TiH_{0.8}$ systems. The absorption spectra at the Ce L_3 edge provides a unique tool to study the valence fluctuation behavior. Indeed, in mixed-valence materials due to the mixing of two configurations in the initial state, $4f^n$ and $4f^{n+1}$, the main line at the L_3 edge shows a characteristic double-peak profile corresponding to the superposition of the atomic $2p \rightarrow 5d$ transition (white line) for each ground state configuration. The white line corresponding to the $4f^{n+1}$ configuration is shifted to lower energy with respect to that of the $4f^n$ due to the screening of the additional $4f$ electron.[29] The two atomic excitations can be resolved because the time scale of the absorption process is two to three orders of magnitude smaller than that associated with the valence fluctuation.[30] Hence, treating the L_3 absorption as a single-particle process and neglecting final state effects, the fractional occupation of the $4f$ configurations in the initial state can be estimated from the intensity ratio of the two white lines that weight the intensity in the final state.[31]

Within this well-established framework, an estimate for the cerium valence was extracted from normalized spectra through a deconvolution model which uses arctangent functions to describe the transitions into the continuum states and Lorentzian functions to take account of the $5d$ states.[31,32] The deconvolution process was performed using a least squares fitting procedure to fit the normalized spectra to the expression

$$F(E) = B_0 + B_1 E + \frac{(\frac{\Gamma}{2})^2 A_1}{(E-E_1)^2 + (\frac{\Gamma}{2})^2} + \frac{(\frac{\Gamma}{2})^2 A_2}{(E-E_2)^2 + (\frac{\Gamma}{2})^2} + \frac{A_1}{A_1 + A_2}\left\{\frac{1}{2} + \frac{1}{\pi}\arctan\left[\frac{E-(E_1+\delta)}{\frac{\Gamma}{2}}\right]\right\} + \left\{1 - \frac{A_1}{A_1 + A_2}\right\}\left\{\frac{1}{2} + \frac{1}{\pi}\arctan\left[\frac{E-(E_2+\delta)}{\frac{\Gamma}{2}}\right]\right\}, \quad (1)$$

where E is the photon energy; E_1 and E_2 are the first accessible $5d$ states in $4f^1$ and $4f^0$ configurations, respectively; Γ is the core-hole lifetime for the considered transition; δ is the shift between the onset of the continuum and bound state transitions; B_0 and B_1 are the coefficients of a linear background; and A_1 and A_2 describe the relative weight of the two configurations.[32,33]

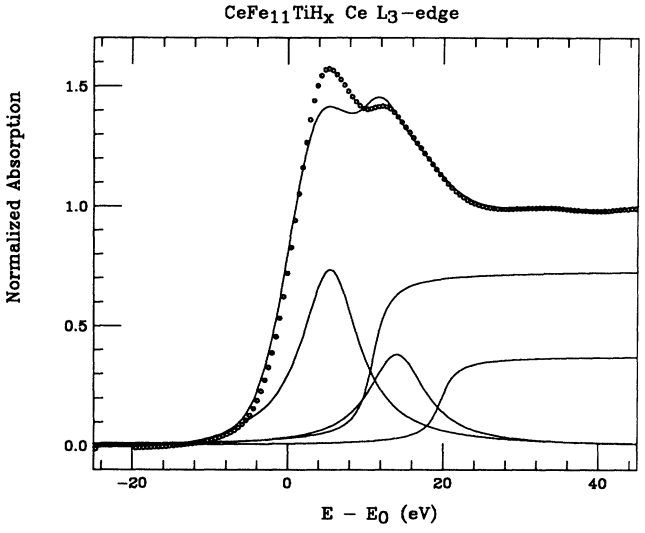

FIG. 4. Deconvolution of the Ce L_3-edge absorption spectrum in the $CeFe_{11}TiH_x$ systems prior (solid line) and after the hydrogen absorption (dots). The deconvolution has been performed including two arctangent and two Lorentzian functions according to Eq. (1) in the text.

Figure 4 shows the deconvolution of the cerium L_3-absorption spectra for $CeFe_{11}Ti$ and $CeFe_{11}TiH_{0.8}$ systems. By this procedure valences of 3.33 ± 0.02 in the case of the pure $CeFe_{11}Ti$ alloy that is reduced to 3.26 ± 0.02 for the hydride derivative are obtained. This weak variation points out that the mixed-valence electronic state of Ce in $CeFe_{11}Ti$ is preserved upon hydrogen absorption. As a consequence, from our data any explanation associating the change in the magnetic properties to the existence, in this crystallographic structure, of nonmagnetic (Ce^{4+}) ions able to collapse in a magnetic (Ce^{3+}) γ-like phase appears not reliable.

C. Ce L_1-edge and Fe, Ti K-edge XANES study

While from the XANES investigation at the Ce L_3 edge the hypothesis of a nonmagnetic (Ce^{4+}) to magnetic (Ce^{3+}) transition cannot be supported, as discussed above, the attribution of the T_c increase upon hydriding to a reduction of the negative exchange interactions among the closest Fe ions triggered by the expansion of the lattice parameters cannot be ruled out also if this explanation seems to be an oversimplification as noted by Herbst.[34] Nevertheless, the changes in the magnetic properties are more likely a consequence of an electronic

effect induced by hydrogen.

To assess this possibility and to improve the description of the empty density of states above the Fermi level in these systems, we performed absorption experiments at the Fe and Ti K edge and at the Ce L_1 edge. In fact, since each absorption edge is sensitive to the local and partial empty density of states of a given symmetry around the selected atomic species, XAS represents an invaluable tool to have a deeper insight on the influence of hydrogen into the electronic density of these complex systems. A comparison of K-iron-edge XANES spectra in $CeFe_{11}Ti$ and its hydride derivative is shown in Fig. 5. Differences between the normalized spectra are observed at the edge region where the shoulderlike feature at the absorption threshold decreases upon hydrogen uptake. The weak variation of the intensity indicates a decrease of the local density of empty p states around the iron site, whereas the shift of the edge toward higher energy suggests a higher localized character of the iron atom that may be associated with a small shift of the Fermi energy of the system. The lack of differences in the near-edge structure mainly formed by multiple scattering resonances, which are very sensitive to the atomic environment around the absorbing atom,[35] represents a nice confirmation of the major role played by the electronic impact of hydrogen over the structural modifications induced.

Both experimental effects are consistent with an electronic transfer from hydrogen to the Fe $3d$ subbands, resulting in a progressive filling of the Fe $3d$ band and the reduction of the mixing between the sp and $3d$ bands. Consequently, the higher localization of the $3d$ band leads to a small enhancement of the overall iron sublattice magnetization. In full agreement with the above discussion, XANES spectra at the Ti K edge in both $CeFe_{11}Ti$ and $CeFe_{11}TiH_x$, reported in Fig. 6, do not exhibit any observable difference, or electronic or structural, as expected if the hydrogen absorption takes place on the $2b$ sites surrounded only by Fe and Ce atoms. Moreover, important information concerning the hydrogen-absorption process and its role in the Ce-Fe hybridization can be obtained looking at the XANES spectra at the Ce L_1 edge shown in Fig. 7. Because of the local site sensitivity of the XAS technique, the excitation from $2s$ core levels (L_1) probes only the local density of the empty p states. In the case of rare earths empty p states are strongly hybridized with the outer s and d continuum states. The L_1 spectra in metallic rare-earth compounds generally exhibit a characteristic shoulder at the threshold. This feature reflects the high density of empty $5d$

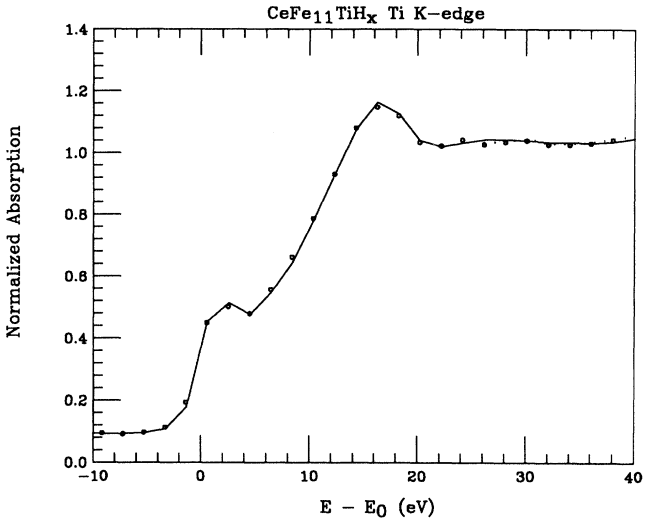

FIG. 6. Comparison between the experimental XANES spectra at the titanium K edge in the case of $CeFe_{11}TiH_{0.8}$ (dots) and $CeFe_{11}Ti$ (solid line) recorded at room temperature.

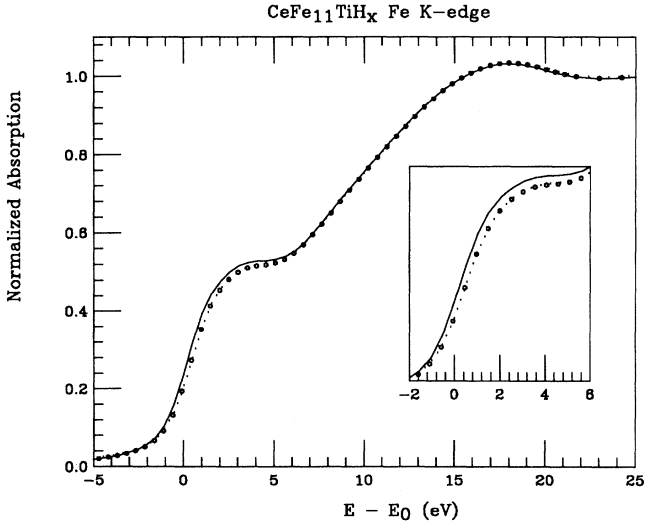

FIG. 5. Comparison between the experimental XANES spectra at the Fe K edge in the case of $CeFe_{11}TiH_{0.8}$ (dots) and $CeFe_{11}Ti$ (solid line).

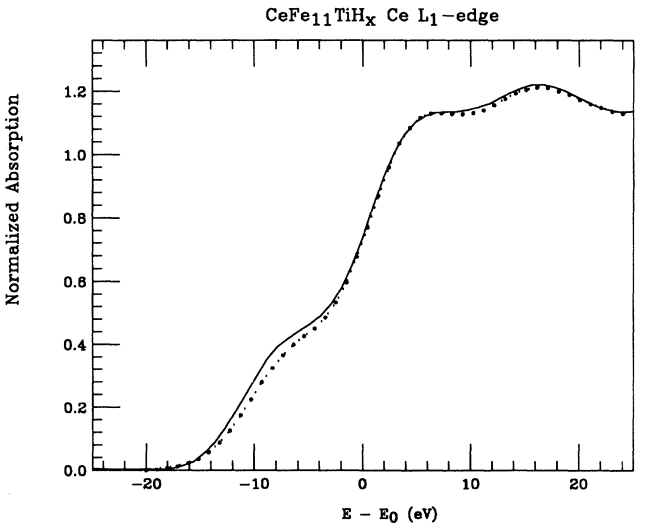

FIG. 7. Comparison between the experimental XANES spectra at the cerium L_1 edge in the case of $CeFe_{11}TiH_{0.8}$ (dots) and $CeFe_{11}Ti$ (solid line).

states via hybridization of the $R(p)$ and $R(5d)$ empty states. Moreover, because of the strong hybridization between rare-earth $5d$ and Fe $3d$ orbitals, L_1-absorption spectra provide a unique insight to study the behavior of the $R(5d)$-Fe($3d$) hybridization upon hydriding. The intensity of the double-staircase feature at the threshold strongly diminishes in $CeFe_{11}TiH_{0.8}$, supporting the hypothesis of a mechanism increasing the localization of the $5d$ band at the rare-earth site. This process reduces the $R(5d)$-Fe($3d$) overlap that determines the interplay between the two magnetic sublattices. This description is consistent with the trend observed at the Fe K-edge XANES spectra. Because the $R(4f)$-Fe($3d$) exchange coupling proceeds via rare-earth $5d$ electrons, a weakening of the R-Fe interaction is expected from our data.

D. XCMD study in $CeFe_{11}TiH_x$ systems

In the previous discussion we emphasized that two mechanisms play a major role in the behavior of $CeFe_{11}Ti$ and $CeFe_{11}TiH_x$ systems. The first one is the structural modification associated with the hydrogen absorption and the second is related to the change with electronic correlation among Fe and Ce atoms. These two mechanisms are certainly correlated because of the role played by the conduction electrons in the hybridization between the Fe and Ce bands which tunes the magnetic properties of these systems. Additional information could then be achieved by using the x-ray-circular-magnetic-dichroism (XCMD) technique. In XCMD experiments, one detects the spin-dependent absorption cross section on a given atomic specie in a material with a net magnetization.[36,37] Actually, in this way the spin polarization of empty states of a given symmetry near the Fermi level, via dipolar selection rules, can be probed by selecting the initial state. Consequently, the capability of XCMD to probe directly the rare-earth $5d$ conduction band by exciting $2p$ core electrons has been explored. This possibility is of fundamental interest because these conduction electrons are very difficult to characterize magnetically since their response to the magnetic probes is generally small compared to the prominent signal given by the narrow bands.

To this end we have performed XCMD measurements at the Ce $L_{2,3}$ edges and at the Fe K edge in $CeFe_{11}Ti$ and $CeFe_{11}TiH_x$ systems. The spin-dependent absorption coefficient is given by the difference of the absorption coefficient $\mu_c = (\mu^- - \mu^+)$ for parallel μ^+ and antiparallel μ^- orientations of the photon spin and the magnetic field applied to the sample. Experimental XCMD spectra were normalized to the averaged absorption coefficient at high energy, μ_0, so that $\mu_c(E)/\mu_0 = [\mu^-(E) - \mu^+(E)]/\mu_0$ corresponds to the thickness-independent spin-dependent absorption coefficient. In our case, the origin of the energy scale was chosen at the inflection point of the absorption edge.

The room temperature XCMD spectra obtained at the Fe K edge in the case of $CeFe_{11}Ti$ and $CeFe_{11}TiH_x$ are shown in Fig. 8 and compared to that of elemental iron. For $3d$ transition metals the K-edge XCMD signal probes the polarization of the $4p$ orbitals at the iron site because

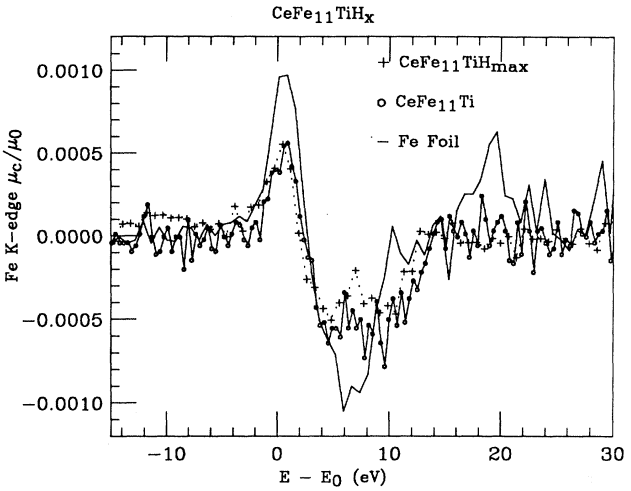

FIG. 8. Fe K-edge XCMD signals recorded at room temperature for iron metal (solid line), $CeFe_{11}Ti$ (o), and $CeFe_{11}TiH_x$ (+).

of the dipole selection rules, implying transitions from the $1s$ core state to the $4p$ conduction band. Moreover, the direction of the magnetic moment on iron atoms relative to the net magnetization of the sample is directly obtained.[38]

However, the relationship between the XCMD signal at the K edge and the magnetic properties of the system is a hard task. In fact, spin-orbit coupling is absent in the initial state so that XCMD is only due to spin-orbit coupling in the final state on the absorbing site. Moreover, the weights of the spin-dependent absorption cross section for transitions towards spin-up (-down) $4p$ states are energy dependent and can even reverse sign.[38] As a result, XCMD effects at the K edge do not immediately lead to direct information on the local magnetic moments. However, in the case of iron metal it was found that the spin splitting of the final p-projected states accounts for the spin dependence of the XCMD at the K edge.[38] Notwithstanding, the correlation between the experimental XCMD spectra and the relative spin polarization of the final empty states can strongly differ within the $3d$ row; an investigation of the spin polarization of the p orbitals may be possible using carefully chosen reference compounds.[39] Taking into consideration the above remarks, it is possible to extract valuable information from the comparison of the Fe K-edge signal in $CeFe_{11}Ti$ to that of iron metal that, as shown in Fig. 8, exhibits a close similarity. The energy splitting of the spin-up and spin-down components of the final p-projected states presents in both cases a positive peak centered at the energy origin, $\simeq 5$ eV wide, followed in energy by a broader dip of negative sign, $\simeq 10$ eV. The similarity of the Fe $4p$ density of states, as probed by the photoelectron, indicates that the impact of additional charge transfer from the rare earth to the conduction bands has no remarkable effect at the Fe sites. Furthermore, the sign of the XCMD signal indicates that the majority of $4p$ spins are parallel to the applied field direction, as expected if the

Fe $4p$ spins are antiferromagnetically coupled to the $3d$ spins.[38]

The intensity ratio between the XCMD signals for iron metal and that of $CeFe_{11}Ti$ is $\simeq 1.6$. This value agrees with that of 1.45 derived from the ratio of the Fe magnetic moment at room temperature in iron metal, $2.17\mu_B$,[40] and in $YFe_{11}Ti$, 1.51 μ_B.[23] Moreover, comparison of the XCMD signals for $CeFe_{11}Ti$ and its hydride derivative does not show any appreciable difference beyond the signal-to-noise ratio, neither in intensity nor in shape, in good agreement with the extremely small 4% enhancement of the Fe magnetic moment upon hydriding.[23]

A similar comparison has been carried out for the XCMD spectra at the Ce $L_{2,3}$ edges, shown in Fig. 9 and Fig. 10. The L_2- and L_3-absorption spectra are sensitive to the $d_{3/2}$ and $d_{5/2}$ final state densities, respectively. Because of the existence of spin-orbit coupling in the initial state, XCMD spectra are directly related to the spin polarization of the final d states projected on the Ce site. This fact makes it possible to relate the dichroic signal to the magnetic moment carried by the $5d$ electrons. Recently, Brouder and Hikam,[38] by using the spin-dependent local density approximation and the multiple scattering theory, have developed a model that gives an account of XCMD in itinerant magnetic materials. According to it, the XCMD signal at the $L_{2,3}$ edges can be written, respectively, as

$$\Delta\sigma_{L_2} = \frac{\sigma^+(\mathbf{B}) - \sigma^-(\mathbf{B})}{\sigma^+(\mathbf{B}) + \sigma^-(\mathbf{B})} = \frac{\sigma^{\downarrow}_{21/2} - \sigma^{\uparrow}_{21/2}}{2(\sigma^{\downarrow}_{21/2} + \sigma^{\uparrow}_{21/2})} , \quad (2)$$

$$\Delta\sigma_{L_3} = \frac{\sigma^{\uparrow}_{23/2} - \sigma^{\downarrow}_{23/2}}{4(\sigma^{\downarrow}_{23/2} + \sigma^{\uparrow}_{23/2})} , \quad (3)$$

where $\sigma^{\uparrow(\downarrow)}_{2j}$ holds for the reduced transition probability towards up (down) spins. Furthermore, by assuming that

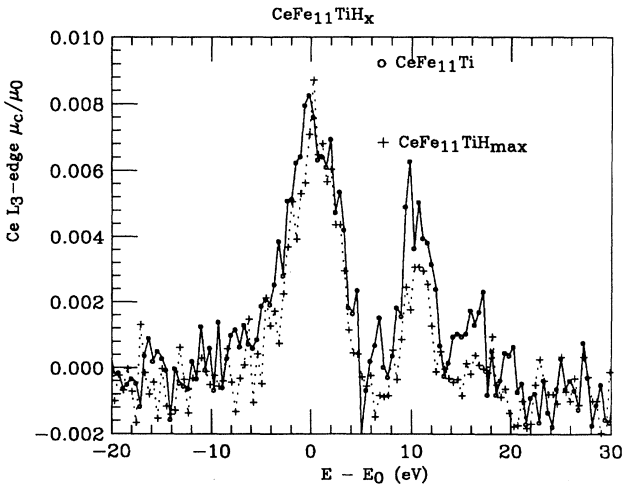

FIG. 9. Ce L_2-edge XCMD signal recorded at room temperature in the case of $CeFe_{11}Ti$ (o) and $CeFe_{11}TiH_x$ (+).

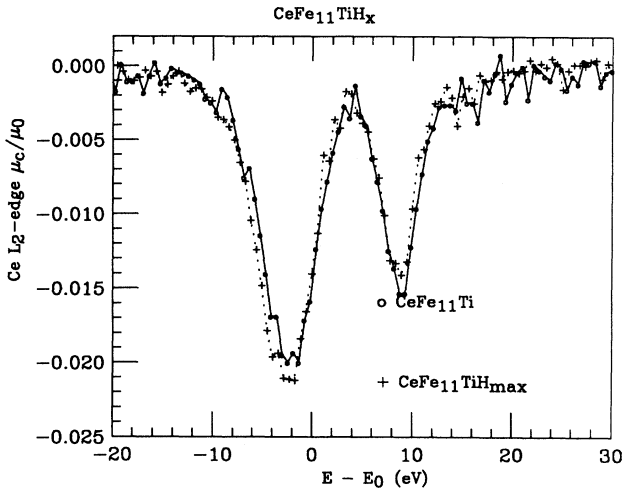

FIG. 10. Ce L_3-edge XCMD signal recorded at room temperature in the case of $CeFe_{11}Ti$ (o), and $CeFe_{11}TiH_x$ (+).

$\sigma^s_{23/2} \simeq \sigma^s_{21/2}$ the relationship between the two edges is given by

$$\left[\frac{\sigma^+ - \sigma^-}{\sigma^+ + \sigma^-}\right]_{L_{II}} = -2\left[\frac{\sigma^+ - \sigma^-}{\sigma^+ + \sigma^-}\right]_{L_{III}} . \quad (4)$$

Thus, the analysis of the XCMD spectra would lead to a direct determination of the sign of the magnetic coupling between the Ce $5d$ spins and the Fe $3d$ spins.

The XCMD spectra at the $L_{2,3}$ edges of Ce in $CeFe_{11}Ti$ and $CeFe_{11}TiH_x$ are characterized by exhibiting a double-peak structure. This feature resembles the existence of configurational mixing $\alpha f^1 + \beta f^0$ in the ground state, in a manner identical to that of the polarization-averaged XAS spectra; see Fig. 4. In fact, the energy splitting of the two XCMD maxima, $\simeq$11 eV, matches well the energy separation of the two Lorentzian functions obtained from the deconvolution of the XANES spectra. It is important to note here that the energy separation of the two maxima in the conventional XANES spectra, Fig. 4, differs from that of the two Lorentzian functions because of the existence of the overimposed transitions to the continuum, treated as arctan functions in the deconvolution model of Eq. (1). On the contrary, the full width at half-maximum (FWHM) of the higher energy peak in the XCMD signals, assigned to the $4f^0$ component, is only 4 eV in contrast to that of 7 eV for the $4f^1$ component, as previously noted by Giorgetti *et al.*[41] for different cerium intermetallic compounds.

The origin of this effect cannot be simply assigned as due to a different core-hole lifetime for the $2p \rightarrow 5d$ transition, Γ, for each of the two components, f^1 and f^0, of the initial state. In fact, the difference found, 3 eV, largely exceeds that derived from Γ values for such transition in pure f^1 and f^0 configurations.[42] In addition, comparing present data and those of Giorgetti *et al.*[41] this difference seems to be constant at both the L_2 and L_3 edges. This result is most likely related to differences in the conduction bandwidth and in the density

of $5d$ states above the Fermi level associated with each electronic configuration. In this sense, the existence of a localized $4f$ electron, $4f^1$ configuration, gives rise to a coupling with the $5d$ band that takes place mainly within the rare-earth atom because the limited range of the $4f$ wave function. Consequently, the $5d$ density of states is more localized on the rare-earth site than if the $4f$ states carry an itinerant character.[43] Making a parallel to the character of each of the two electronic configurations in the Ce ground state a higher width of the XCMD signal for the f^1 component would be expected as experimentally observed.

As discussed above, the XCMD spectra at the Ce L edges carry information about the relative orientation of the $5d$ spins and the external applied field. In the case of $CeFe_{11}Ti$ and its hydride derivative XCMD signals are negative at the L_2 edge and positive at the L_3 edge. The branching ratio is $\simeq -2.4$, close to the -2 value predicted by Eq. (4), indicating that the $5d$ magnetic moment is almost of spin character.[41] This result indicates that the spin of the $5d$ states is parallel to the external field, i.e., to sample magnetization. According to the simplified model of the level densities for rare-earth transition-metal intermetallic compounds developed by Johanson *et al.*,[43] the energy distance between the bonding and antibonding $3d$-$5d$ subbands is different for the two spin directions and therefore $3d$-$5d$ hybridization is different for the majority and minority spins. In the case that no localized $4f$ magnetic moment is present in the system, the occupation of the spin down (minority) of the $5d$ part exceeds that of the majority spin one in its turn hybridized to the majority spin Fe $3d$ band. Consequently there is a total $5d$ spin moment on the rare earth coupled antiferromagnetically to the Fe $3d$ moment.

In the case of $CeFe_{11}Ti$ and $CeFe_{11}TiH_x$ systems, XCMD spectra fully support the above picture, indicating both the existence of an ordered net $5d$ magnetic moment at the Ce sites as well as its antiferromagnetic coupling to the Fe $3d$ magnetic moment. This trend agrees with Campbell's indirect exchange hypothesis formulated to account for the magnetic coupling in rare-earth transition-metal compounds.[44] XCMD results are also in agreement with recent electronic structure calculations performed for the RFe_{12} systems, R=Y, Ce, and Gd, yielding that although the number of occupied states in the s and p bands of the R atoms is almost the same for both spin states, the down spins are more than the up spins in the d bands. Therefore the spin polarization is small for the s and p states, but the magnetic moment due to the d spin polarization is appreciable and antiparallel to those of the irons.[45–47]

Finally, the intensity ratio of the XCMD signals at the Ce L edges yields the same valency for Ce as derived from the analyses of the XAS spectra. Upon hydrogen absorption a reinforcement of the f^1 component at the expense of the f^0 one is observed, but the sign of the signal does not change. However, for systems in which a localized Ce $4f$ magnetic moment is present (i.e., pure f^1 electronic configuration) such as $CeFe_2H_x$, the sign of XCMD signals at the L edges is just the opposite of that observed in mixed-valence Ce materials such as $CeFe_{11}Ti$ and $CeFe_{11}TiH_x$.[41] This result is extremely significant, indicating that in these systems no localized $4f$ moment arises at the Ce sites upon hydriding.

IV. CONCLUSIONS

The interpretation of the x-ray-absorption spectra recorded at different atomic species (Ce, Ti, and Fe) at different absorption edges leads to a better understanding of the origin of the magnetic changes occurring upon hydriding in $RFe_{11}Ti$ systems.

From the EXAFS analysis of the spectra measured at the transition-metal sites, the crystallographic position occupied by hydrogen has been inferred to be the octahedral $2b$ site. The structural modifications induced by hydrogen are present but negligible, addressing the rise in the magnetic ordering temperature to the enhancement of the iron $3d$-$3d$ exchange. This effect reflects the increase of localization of the conduction electrons at the iron sites, as due to the electronic transfer from the H atoms to the iron $3d$ subbands. This mechanism produces an increment of the overall Fe sublattice magnetization that is supported by the XAS spectra at the K edge of Fe and Ti, and by the L_1 edge of cerium. From L_3 XAS spectra a mixing of configurations is detected for cerium and also a very small change of the mixed valence upon H_2 absorption is observed. This result ruled out the presence of pure Ce^{3+} configuration in the hydride derivative. Moreover, the simultaneous analysis of the XAS and XCMD data indicates that the changes of the magnetic properties upon hydriding are mainly associated with the variation of the $3d$(Fe)-$5d$(Ce) hybridization rather than with the induction of a localized $4f$ magnetic moment at the Ce site.

ACKNOWLEDGMENTS

This work was partially supported by DGICYT MAT93-0240C04 and EEC ERBCHRXCT920034 grants. One of us (J.Ch.) acknowledges partial support from the Ministerio de Educación y Ciencia of Spain (Programa Sectorial de Promoción General del Conocimiento, Solicitud de Ayuda para la Utilización de Recursos Científicos).

[1] J.J. Croat, J.F. Herbst, R.W. Lee, and F.E. Pinkerton, Appl. Phys. Lett. **44**, 148 (1984).

[2] M. Sagawa, S. Fujimura, N. Togawa, H. Yamamoto, and Y. Matsuura, J. Appl. Phys. **55**, 2083 (1984).

[3] D.B. De Mooij and K.H.J. Buschow, Philips J. Res. **42**, 246 (1987).

[4] F.R. De Boer, Ying-Kai Hung, D.B. De Mooij, and K.H.J. Buschow, J. Less-Common Met. **135**, 199 (1987).

[5]K.H.J. Buschow, D.B. De Mooij, M. Brouha, H.H.A. Smit, and R.C. Thiel, IEEE Trans. Magn. **MAG-24**, 1161 (1988).
[6]Xian-Zhong Wang, B. Chevalier, T. Berlureau, J. Etouerneau, J.M.D. Coey, and J.M. Cadogan, J. Less-Common Met. **138**, 235 (1988).
[7]Bo-Ping Hu, Hong-Shuo Li, J.P. Gavigan, and J.M.D. Coey, J. Phys. Condens. Matter **1**, 755 (1989).
[8]Y.C. Yang, X.D. Zhang, S.I. Ge, Q. Pan, L.S. Kong, and H. Li, J. Appl. Phys. **70**, 6001 (1991).
[9]P. Dalmas de Reotier, D. Fruchart, L. Pontonnier, F. Vaillant, P. Wolfers, A. Yaouanc, J. M. Coey, R. Fruchart, and Ph. L'Heritier, J. Less-Common Met. **129**, 133 (1987).
[10]O. Isnard, S. Miraglia, J.L. Soubeyroux, D. Fruchart, and A. Stergiou, J. Less-Common Met. **162**, 273 (1990).
[11]D. Fruchart, F. Vaillant, A. Yaouanc, J. M. Coey, R. Fruchart, Ph. L'Heritier, T. Riesterer, J. Osterwalder, and L. Schlapbach, J. Less-Common Met. **130**, 97 (1987).
[12]J. Chaboy, J. Garcia, A. Marcelli, O. Isnard, S. Miraglia, and D. Fruchart, J. Magn. Magn. Mater. **104-107**, 1171 (1992).
[13]L. Bozukov, A. Apostolov, and M. Stoytchev, J. Magn. Magn. Mater. **101**, 355 (1991).
[14]A. Apostolov, L. Bozukov, and N. Stanev, J. Magn. Magn. Mater. **83**, 55 (1990).
[15]F. Baudelet, E. Dartyge, G. Krill, J.P. Kappler, C. Brouder, M. Piecuch, and A. Fontaine, Phys. Rev. B **43**, 5857 (1991).
[16]B. Lengeler and P. Eisenberger, Phys. Rev. B **21**, 4507 (1980).
[17]C.A. Ashley and S. Doniach, Phys. Rev. B **11**, 1279 (1975).
[18]S. Obbade, S. Miraglia, D. Fruchart, P. L'Heritier, and A. Barlet, C. R. Acad. Sci. Paris **307**, 889 (1988); S. Obbade, S. Miraglia, D. Fruchart, and P. L'Heritier, Z. Phys. Chem. **163**, 162 (1989); S. Obbade, Ph.D. thesis, Grenoble University, 1992.
[19]E. Tomey, M. Bacmann, D. Fruchart, S. Miraglia, J.L. Soubeyroux, D. Gignoux, and E. Palacios, IEEE Trans. Magn. **MAG-30**, 687 (1994).
[20]J.J. Rehr, J. Mustre de Leon, S.I. Zabinsky, and R.C. Albers, J. Am. Chem. Soc. **113**, 5135 (1991); J. Mustre de Leon, J.J. Rehr, S.I. Zabinsky, and R.C. Albers, Phys. Rev. B **44**, 4146 (1991).
[21]M. Sanchez del Rio and J. Chaboy, Comput. Chem. (to be published).
[22]D. Givord and R. Lemaire, IEEE Trans. Magn. **MAG-10**, 109 (1974).
[23]L.Y. Zhang and W.E. Wallace, J. Less-Common Met. **149**, 371 (1989).
[24]W.E. Wallace, Prog. Solid Chem. **16**, 127 (1986).
[25]L.Y. Zhang, F. Pourarian, and W.E. Wallace, J. Magn. Magn. Mater. **71**, 203 (1988).
[26]O. Isnard, S. Miraglia, D. Fruchart, and J. Deportes, J. Magn. Magn. Mater. **103**, 157 (1990).
[27]S. Miraglia, M. Anne, H. Vincent, D. Fruchart, J. M. Laurant, and M. Rossignol, J. Less-Common Met. **153**, 51 (1989).
[28]D. Wohlleben and J. Röhler, J. Appl. Phys. **55**, 1904 (1984).
[29]S.M. Blokhin and E.Ye. Vaynshteyn, Fiz. Met. Metalloved. **19**, 371 (1965) [Phys. Met. Metallogr. (USSR) **19**, 49 (1965)].
[30]H. Launois, M. Rawiso, E. Holland-Moritz, R. Pott, and D. Wohlleben, Phys. Rev. Lett. **44**, 1271 (1980).
[31]J. Röhler, in *Handbook on the Physics and Chemistry of Rare Earths*, edited by K.A. Gschneider, Jr., L. Eyring, and S. Hufner (Elsevier Science, New York, 1987), Vol. 10, Chap. 71.
[32]J. Röhler, J. Magn. Magn. Mater. **47&48**, 175 (1985).
[33]J. Chaboy, Ph.D. thesis, Zaragoza University, 1991.
[34]J.F. Herbst, Rev. Mod. Phys. **63**, 819 (1991).
[35]See, for example, A. Bianconi, in *X-Ray Absorption: Principles, Applications, Techniques of EXAFS, SEXAFS, XANES*, edited by R. Prinz and D. Koningsberger (Wiley & Sons, New York, 1988) and references therein.
[36]G. Schütz, W. Wagner, W. Wilhelm, P. Kienle, R. Zeller, R. Frahm, and G. Materlik, Phys. Rev. Lett. **58**, 737 (1987).
[37]G. Schütz, M. Knulle, R. Wienke, W. Wilhelm, W. Wagner, P. Kienle, and R. Frahm, Z. Phys. B **73**, 67 (1988).
[38]C. Brouder and M. Hikam, Phys. Rev. B **43**, 3089 (1991).
[39]S. Stähler, G. Schütz, and H. Ebert, Phys. Rev. B **47**, 818 (1993).
[40]J. Crangle and G.M. Goodman, Proc. R. Soc. London Ser. A **321**, 477 (1971).
[41]C. Giorgetti, S. Pizzini, E. Dartyge, A. Fontaine, F. Baudelet, C. Brouder, Ph. Bauer, G. Krill, S. Miraglia, D. Fruchart, and J.P. Kappler, Phys. Rev. B **48**, 12 732 (1993).
[42]K.D. Sevier, *Low Energy Electron Spectrometry* (Wiley Interscience, Chichester, UK, 1972) (estimates of Γ in pure f^0 configuration have been derived from La and Lu).
[43]B. Johansson, L. Nordström, O. Eriksson, and M.S.S. Brooks, Phys. Scr. T **39**, 100 (1991).
[44]I.A. Campbell, J. Phys. F **2**, L47 (1972).
[45]S. Asano, S. Ishida, and S. Fujii, Physica B **190**, 155 (1993).
[46]O. Eriksson, L. Nördstrom, M.S.S. Brooks, and B. Johansson, Phys. Rev. Lett. **60**, 2523 (1988).
[47]L. Nördstrom, O. Eriksson, M.S.S. Brooks, and B. Johansson, Phys. Rev. B **41**, 9111 (1990).